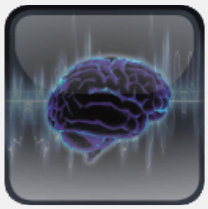

Ketogenic Diet and Metabolic Therapies: Expanded Roles in Health and Disease

Edited by Susan A Masino, PHD

Publisher: Oxford University Press
Print Publication Date: Oct 2016
Print ISBN-13: 9780190497996
Published online: Nov 2016
DOI: 10.1093/med/9780190497996.001.0001

Mitigation of Damage from Reactive Oxygen Species and Ionizing Radiation by Ketone Body Esters

Chapter:

Mitigation of Damage from Reactive Oxygen Species and Ionizing Radiation by Ketone Body Esters

Author(s):

William Curtis, Martin Kemper, Alexandra Miller, Robert Pawlosky, M. Todd King, and Richard L. Veech

DOI: 10.1093/med/9780190497996.003.0027

Introduction

Free radicals play an important role in a number of chronic degenerative diseases including autoimmune disorders, aging (Harman, 1956), cataracts, rheumatoid arthritis, Parkinson’s disease (Kashiwaya et al., 2000), cardiovascular disease, and other neurodegenerative diseases (Pham-Huy et al., 2008). However, the pathophysiology of these diseases can be complex. The simplest form of ROS-induced disease is radiation sickness.

Origins of Reactive Oxygen and Nitrogen Species

Reactive oxygen species (ROS) and reactive nitrogen species (RNS) arise from numerous sources including cellular metabolism, ionizing radiation, and various enzymes. Once created, individual ROS and RNS participate in a cascade of interconversions (Figure **27.1**) both enzymatic and not, ultimately being detoxified by being converted into inert molecules or by damaging various biomolecules.

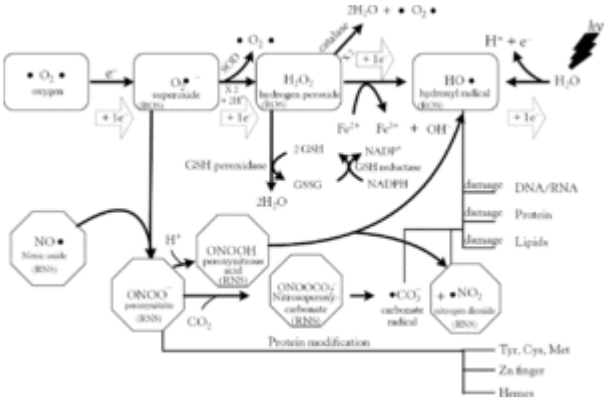

Figure 27.1
The origin, reactions, and target molecules of reactive oxygen species (ROS) and reactive nitrogen species (RNS) are shown. Free radicals include superoxide, hydroxyl and nitric oxide, carbonate radical, and nitrogen dioxide. The oxidation steps show the sequence of four single-electron reductions (addition of one electron) from oxygen to superoxide to peroxide to hydroxyl to water. The outlined arrow $+1e^-$ indicates reduction. The reaction of ionizing radiation with water is represented by $h\nu$, where h is Planck's constant and the Greek letter ν is the frequency, which gives the energy of the electromagnetic radiation by $E = h\nu$ where $h = 6.626 \times 10–34$ Js. Abbreviations: e^- —electron, SOD—superoxide dismutase, GSH—glutathione, GSSG—glutathione disulfide, TYR—tyrosine, MET—methionine, CYS—cysteine.

Basal production of ROS occurs in the mitochondria as a byproduct of normal metabolism by the spontaneous oxidation of coenzyme Q semiquinone by oxygen, creating superoxide ($O_2\bullet^-$) (Chance et al., 1979).

$$Q\bullet^- + O_2 \rightarrow O_2\bullet^- + Q$$

Another common origin of ROS is radiation; ionizing radiation with energy ($h\nu$) above 33eV can ionize water, which makes up the vast majority of human cell volume. This process occurs with many radiation types including particles (e.g., α or β), electromagnetic (e.g., γ or X), and

neutrons. Radiation of sufficient energy will split water into a hydroxyl radical (HO•), H^+, and a free electron, e^-. These three species interact with a variety of other molecules to form the cascade of RNS and ROS shown in Figure **27.1**.

Superoxide can also be generated without radiation by NADPH oxidases (NOXs) in white blood cells in response to pathogens (Bedard and Krause, 2007) or as an inducible response to inflammation and cellular stress. Enzymes producing ROS are also induced after exposure to radiation, particularly the NOX family members DUOX 1 and 2, which continue producing superoxide for a number of days post radiation (Ameziane-El-Hassani et al., 2015). This prolonged ROS production leaves a therapeutic window for post-radiation treatment that targets these molecules.

Numerous other enzymes produce other types of ROS as part of their normal function, such as monoamine oxidase (MAO) (EC 1.4.3.4), an enzyme integral in monoaminergic neurotransmission and xenobiotic metabolism. This enzyme produces hydrogen peroxide as part of its breakdown of monoamines, such as dopamine in this reaction: Dopamine + H_2O +O_2 → Dopaldehyde + NH_3 + H_2O_2. This is an important issue in the treatment of Parkinsonian patients, who are often given high doses of L-dopa, which is known to increase ROS load (Acquier et al., 2013) and can lead to further loss of dopaminergic neurons, often seen in patients on high doses of L-dopa (Yamato et al., 2010).

Figure **27.1** provides a roadmap showing the cascade of ROS and RNS. Superoxide plays a central role in the cascade. In the case of radiation, superoxide results from the free electron combining with oxygen. The enzyme superoxide dismutase (SOD) catalyzes a reaction where two superoxide ions react to produce oxygen and hydrogen peroxide. The hydrogen peroxide can decompose to hydroxyl radical and hydroxide in the presence of iron and other metals via the Fenton reaction. Superoxide reacts with nitric oxide (NO) to produce peroxynitrite and begins the cascade of RNS. The reaction of NO with superoxide is diffusion limited and nonenzymatic. This is especially problematic as NO is uncharged, enabling it to pass quickly through cellular membranes, and possesses a relatively long half-life. The kinetics of the reaction of NO with superoxide make the production of peroxynitrite inevitable whenever NO is produced within a few cell diameters of superoxide (Pacher et al., 2007). Peroxynitrite in turn can either react directly with CO_2 to form nitrosoperoxycarbonate, which dissociates to form other radical species, or be protonated to form peroxynitrous acid, which dissociates into hydroxyl radical and nitrogen dioxide radical. The formation of hydroxyl

radical from peroxynitrite may contribute more to the formation of free radicals than the iron catalyzed Fenton reaction (Pacher et al., 2007).

Oxygen-containing free radicals and other ROS or their nitrogenous counterparts perform useful functions in cell signaling and physiology (Pham-Huy et al., 2008). While the causes of excessive ROS and RNS in diseases may have complex or indeterminate origins, the exposure to radiation provides a model with a single known initiator. Generation of ROS/RNS is a component of many common diseases including cataracts, rheumatoid arthritis, neurodegenerative diseases such as amyotrophic lateral sclerosis (ALS) and Parkinson's (Kashiwaya et al., 2000) and Alzheimer's disease, cancer (Pham-Huy et al., 2008), and aging (Harman, 1956). Table 27.1 summarizes reactions that generate or destroy RNS and ROS.

Table 27.1 The Generation and Destruction of RNS and ROS

ROS/RNS formation reactions	**ROS/RNS destruction reactions**	**Catalyst**
$H_2O + h\nu \rightarrow HO\bullet + H^+ + e^-$		$h\nu$
$O_2 + e^- \rightarrow O_2\bullet^-$		NOX, xanthine oxidase
$Fe^{2+} + H_2O_2 \rightarrow Fe^{3+} + HO\bullet + OH^-$		spontaneous
$O_2\bullet^- + NO\bullet \rightarrow ONOO^-$		spontaneous
	$HO\bullet + O_2\bullet^- \rightarrow OH^- + O_2$	spontaneous
	$2\ O_2\bullet^- + 2H^+ \rightarrow H_2O_2 + O_2$	Superoxide dismutase
	$2\ H_2O_2 \rightarrow O_2 + 2H_2O$	Catalase
	$2GSH + H_2O_2 \rightarrow GSSG + 2H_2O$	Glutathione peroxidase

Damage Caused by Reactive Oxygen and Nitrogen Species

Free radicals attack nucleic acids, proteins, and lipids indiscriminately. Nucleic acids are attacked either at the sugar (ribose or deoxyribose) or the base that is responsible for pairing. If hydroxyl reacts with the sugar, it results in strand breaks, recombination, chromosomal changes and mutations. If hydroxyl radical reacts with the base, it adds alcohol groups, OH, to the base where none belong and interferes with the hydrogen bonding and fit of the matching base pair, leading to point mutations. Modified guanine interferes with the telomerase binding proteins TRF1 and TRF2 and causes a loss of telomere function, which requires these binding proteins for both the protective shelterin complex and for telomerase to interact with shelterin and extend the telomere (Sfeir, 2012). See for example Figure **27.2**.

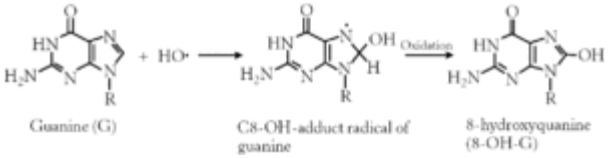

Figure 27.2
Guanine reacts with hydroxyl radical to produce 8-OH-G. There are three guanines in the telomere repeat sequence, TTAGGG, making it vulnerable to oxidative damage. R is deoxyribose.

Proteins have various reactions depending on the amino acid. One that is vulnerable is cysteine. Oxidative stress can cause cysteine on two proteins or within one protein to form a disulfide bridge and change the folding of the protein. This can be reversed as a protein disulfide bond is reduced by thioredoxin reduction reaction shown in Figure **27.4**. However, further oxidation leads to SOH, SO_2H and SO_3H, which makes the protein permanently damaged.

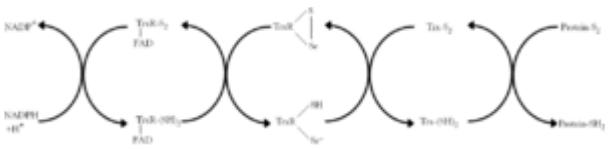

Figure 27.4
Thioredoxin is a family of three proteins in mammals—TrxR1 (cytosolic), TrxR2 (mitochondrial), TrxR3 (testis specific)—that can reduce protein disulfide bonds formed by ROS/RNS damage. Abbreviations: TrxR—thioredoxin, FAD—flavin adenine dinucleotide, S2—disulfide, SH2—two sulfhydryl moieties.

Damage to lipids is primarily to polyunsaturated fatty acids (PUFAs). There are three stages, initiation, propagation, and termination. Initiation causes the PUFA to become a free radical. Propagation generates other free radicals, oxygen is often involved. Oxygen is a dual free radical, and one might draw it as $\bullet O_2 \bullet$ to show the two unpaired electrons. Being a dual radical makes $\bullet O_2 \bullet$ especially reactive with transition metals that are free radicals and also other free radicals. Having the two unpaired electrons allows $\bullet O_2 \bullet$ to propagate damage as in $R\bullet + O_2 \rightarrow ROO\bullet \rightarrow$ further reactions. $NO\bullet$ being a single free radical would result in a terminating reaction with other free radicals as $RS\bullet + NO\bullet \rightarrow RS{-}NO$.

Peroxynitrite ($ONOO^-$) is very reactive but it is not a free radical, therefore it tends to modify proteins on specific residues and motifs such as methionine, tyrosine, zinc fingers, and heme (see Figure **27.1**).

The Role of Reactive Oxygen Species in Aging

In 1956, Denham Harmon, working in the Donner Biophysics Lab at Berkeley, wrote a paper postulating that the process of aging was the result of free radicals produced either endogenously or by environmental sources (Harman, 1956). In 1961 Hayflick and Moorman showed that cultured cells could undergo only a finite number of replications for reasons that were unclear. In 1973 Olovnikov postulated that the end replication of DNA would result in the shortening of that strand at every replication (Olovnikov, 1973). In 1978, Elizabeth Blackburn published a paper describing a special form of DNA at the end of chromosomes, which is the telomere (Blackburn and Gall, 1978). In 1990 it was found that the telomere of human fibroblasts shortened with aging (Harley et al., 1990). This sequence seemed to provide a mechanism to explain the development of senescence, at least in culture.

Cell senescence can be triggered by a number of mechanisms including telomere uncapping, DNA damage, oxidative stress, oncogene activity, lack of nutrients, and other factors via various signaling pathways (Ben-Porath and Weinberg, 2005). A number of studies reported that oxidative stress shortened telomeres (von Zglinicki, 2002). The formation of 8-oxo-guanine lesions in telomeric tandem repeats by ROS-damaged telomeric protein binding to telomeres (Opresko et al., 2005) impaired their functioning, causing replication to cease.

In the absence of disease, ROS damage depends on the rate of metabolism and with it, the rate of ROS production by mitochondria, which roughly correlate with the life span (Speakman, 2005), a phenomenon known as scaling. From these and other observations it was thought that the rate of metabolism inversely correlated with life span and slowing it by measures such as caloric restriction would lengthen life span (Sohal and Weindruch, 1996), in part by limiting mitochondrial ROS generation and hence ROS damage. Studies also appeared which reported that overexpression of the antioxidant enzyme catalase increased life span in transgenic mice (Schriner et al., 2005). Other antioxidant enzymes also increased life span in *Drosophila* (Orr et al., 2013).

The most important system providing antioxidants and defending against ROS is the NADPH defense system described later in this chapter. The preceding reports show that ROS can accelerate telomere shortening, damage DNA directly, induce senescence, and hasten the aging process (Correia-Melo et al., 2014). Suppressing ROS may slow the shortening of telomeres and decrease activation of other mechanisms implicated in the pathology of aging (Harman, 1956, 1981). We postulate that using ketone body esters to suppress ROS would be effective in retarding the aging process itself.

Telomere shortening occurs during normal aging, leading to uncapping, activating senescence and apoptotic programs in tissues with high cell turnover. Rapidly dividing cells—gut, skin, hematopoietic, and immune cells—replicate constantly during life, and aging is visible to anybody in skin as it changes from thick and smooth in youth to thin and wrinkled in the aged. The effects of nuclear radiation are likewise amplified in these tissues, exposure in the range of 2 to 5 Gy suppresses replication of blood and gut cells through generation of ROS, causing death in weeks. In these rapidly dividing cell types, a telomeric process as described by Hayflick could play a more dominant role.

There is, however, another large group of cells that undergo almost no replication after embryonic life. They include heart, skeletal muscle, and

brain cells. The death of these slowly dividing cells does not have a unitary mechanism. The gradual onset of senescence that characterizes normal aging may in part be due to the accumulation of genetic damage over a lifetime (Szilard, 1959).

Mice lacking the gene for dystrophin (MDX) demonstrate little cardiac abnormalities. However, mice in which the mRNA component of telomerase, *mTR*, was deleted show progressive shortening of telomeres with age. Crossing these two strains to form the *mdx/mTR*^{ko} mouse with deleted dystrophin and TERC produced a mouse with heart abnormalities, mitochondrial dysfunction, and oxidative stress with reduced levels of the mitochondrial regulators peroxisome proliferator activated receptor gamma coactivator 1 α and 1 β (PGC1-α and PGC1-β), both reduced by 80%. The pathological changes in hearts of these animals were ameliorated by administration of antioxidants(Mourkioti et al., 2013). These findings show that both mitochondrial ROS production and telomere shortening play a role in the death and dysfunction of non-rapidly dividing cells such as heart cells and that these functional abnormalities induced in *mdx/mTR*^{ko} can be reduced by administration of antioxidants.

The toxicity from radiation is therefore both acute and chronic. Acute death occurs from effects on the central nervous system (CNS) at doses of 20 Gy, or slow, long-term accumulated DNA damage leading to cell death from multiple hits (Szilard, 1959). An earlier speculation by Erwin Schrodinger attributed life to the maintenance of negative entropy by homeostatic processes (Schrodinger, 1944). In this view, aging and death would be the result of an increase in entropy. This general statement without a biochemical or physiological mechanism is of limited practical use, whereas applications of thermodynamics as exemplified by the energetics of the various redox states and the process of oxidative phosphorylation have heuristic value.

How Antioxidants Work

There is a basic pattern to how antioxidant small molecules work. They follow the pattern of reaction shown in Figure **27.3**.

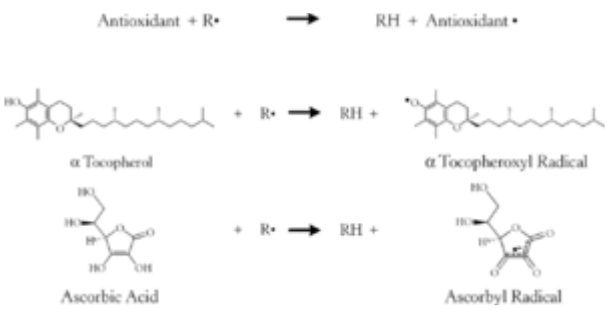

Figure 27.3
The basic pattern of antioxidant reactions results in an antioxidant radical, which must be reduced before it can participate in additional reactions. The antioxidant free radicals are sometimes obscured as they are the first step in a reaction mechanism that may go to other forms.

The antioxidant is oxidized and the free radical is reduced. Why then is it not a problem that the antioxidant has become a free radical? The answer is that the unpaired electron in the now antioxidant radical is delocalized and thus less reactive. This property makes ascorbate and tocopherol distinct from other cellular reducing agents, as they remain stable compounds after a single electron transfer. This is in contrast to glutathione, a powerful and important reducing agent, but one that must transfer two electrons at once to remain stable, as the glutathione radical is highly reactive. Tocopherol is able to transfer a single electron but only a single electron, ascorbate is able to transfer two—and, importantly, two ascorbate radicals are able to react, forming a single molecule of dihydroascorbate and one molecule of ascorbate. Dihydroascorbate in turn is able to accept two electrons from glutathione and be regenerated, bridging single electron redox couples with two electron couples. Glutathione itself is reduced by the free [$NADP^+$]/[NADPH] redox couple. It is important to understand factors controlling the cellular redox states to understand how the antioxidants get recharged (reduced).

The Cellular Redox States Differ from the Standard Redox Potentials

A great deal of confusion in the literature on oxygen free radicals results from the use of tables of standard reduction potentials, ΔE^o, done at pH 7.0 with all reactants at 1 M.

The redox state of the cytoplasmic NAD- couple in vivo was first defined in 1955 by Lynen and his coworkers (Holzer et al., 1956) in yeast by measurement of the ratio of the metabolites [ethanol]/[acetaldehyde] in a reaction brought to near-equilibrium by the very active cytoplasmic

enzyme alcohol dehydrogenase. Soon thereafter it was shown by Bucher and Klingenberg (1958) that the free [NAD^+]/[NADH] in rat liver cytoplasm could be estimated by measurement of either the [lactate]/[pyruvate] or [dihydroxyacetone-P]/ [3-glycerophosphate] ratio. Because of the rapidity with which these cellular redox state estimates change with hypoxia, accurate determinations were facilitated by the development of freeze clamping (Wollenberger et al., 1960). That ratio of [lactate]/[pyruvate] was found to be between 5 and 10, giving a free cytosolic [NAD^+]/[NADH] calculated from the measured Keq of the reaction to be about 1,000 in the fed liver and 250 in a starved liver. Following these principles, in 1967 Krebs and his coworkers (Williamson 1967) showed that the free [NAD^+]/[NADH] ratio in mitochondria could be estimated by measurement of ether the [acetoacetate]/[β-D-hydroxybutyrate] or [α-ketoglutarate]×[NH_4^+]/[glutamate] ratio and the ratio of free mitochondrial [NAD^+]/[NADH] was found to be between 2 to 10. Following a question to Krebs by George Cahill, Krebs assigned Richard Veech to determine the free cytoplasmic [$NADP^+$]/[NADPH] ratio, which was known be used in the reductive synthesis of fats. This ratio was found to be about 0.01 to 0.02 and could be estimated by measurement of [α-ketoglutarate]×[CO_2]/[isocitrate] or several other couples (see Table 27.2) The standard potential of the NAD- couple is about −0.32 V, but these couples have three potentials in the cell depending on the intracellular location of the enzymes involved. The three redox couples have redox potentials appropriate to the metabolic pathways they drive.

Table 27.2 The Activity of NADP-Linked Enzymes in Rat Liver

Enzyme	Activity in µmol/min/g	K_{eq} = Metabolite couple	K_{eq} value
Isocitrate DH EC 1.1.1.41	22	$K_{eq}=\frac{[\alpha KG^{2-}][CO_2][NADPH]}{[Isocitrate^{3-}][NADP^+]}$	1.17 M
Glutathione Reductase EC 1.6.4.2	7	$K_{eq}=\frac{[GSSG][NADPH][H^+]}{[GSH]^2[NADP^+]}$	100×10^{-7} (Scott et al., 1963)
6 P Gluconate DH EC 1.1.1.44	2.8	$K_{eq}=\frac{[Ribulose\ 5P^{2-}][CO_2][NADPH]}{[6P\ Gluconate^{3-}][NADP^+]}$	1.72×10^{-1} M (Villet and Dalziel, 1969)
Glucose 6-P DH EC 1.1.1.49	1.4	Not applicable because of lactonase	
Malic Enzyme EC 1.1.1.39	1.27	$K_{eq}=\frac{[pyruvate^-][CO_2][NADPH]}{[Malate^{2-}][NADP^+]}$	3.44×10^{-2} M

Source: Veech et al. (1969)

First, in cytoplasm, the ΔE of the free NAD- couple is −0.19 V, this smaller potential poising it to receive reducing power from glycolysis. Second, for NAD in mitochondria, it is −0.28 V, allowing for more energy to be available for the electron transport pathway to convert ADP to ATP. Third, the NADP- couple in the cytosol was estimated to be about −0.42 V, the lowest reduction potential in the cell (Krebs & Veech 1969). This strongly reducing potential allows this couple not only to synthesize fats but also to favor the inactivation of oxygen free radicals through the two major intracellular antioxidants, glutathione (GSH) and ascorbic acid (Vitamin C). As these antioxidants are in near equilibrium with the free cytoplasmic [$NADP^+$]/[NADPH] couple, whose large reducing potential favors the reduced, active forms of GSH and Vitamin C (see Table 27.2 for

a list of these redox couples and Figure **27.4** for a diagram of the ROS-quenching reactions driven by the NADP couple).

These major cellular redox states are related to one another through common intermediary metabolites (Bergman et al., 2010; Krebs, 1969) and also to the cellular phosphorylation potential or ATP/ADPxP_i ratio keeping the energy of ATP hydrolysis in the range of −53 to −57 k*J*/mole (Veech et al., 1979). It can be seen that these intracellular redox potentials cannot be inferred by study to the standard potential of redox half reactions, which have led to much confusion in writing about cellular redox potentials (Winterbourn, 2008). This history of the development of the measurement of in vivo redox states has been reviewed (Veech, 2005, 2006).

Measurement of each of the metabolite couples listed in Table 27.2 yields the same value of the free cytosolic [$NADP^+$]/[NADPH] ratio with a redox potential of about −0.4 V, the most negative of any intracellular potential (Krebs, 1969). With small refinements of the Keq, CO_2 concentrations and intracellular metabolite concentrations in the intervening years, the potential of the NADP system is more likely to be in the range of −0.36 to −0.38 V, but is still the most negative potential in the cell.

The formalism to calculate the redox potential in the cell estimated from measured intracellular metabolites and the measured Keq of the reactions involved is as follows. The standard redox potential is derived from the equilibrium constant of the reaction. The standard potential of both the NAD and NADP couples, E^o, is, within experimental error, −0.32 V (Burton, 1974).

The redox potential within the cell is calculated at follows (Veech, 2005):

$$E_{NAD/NADH} = E^{o}_{NAD/NADH} + \frac{RT}{nF}\ln\left(\frac{NAD^+}{NADH}\right)$$

Eqn 1

Where R = 8.1345 × 10^{-3} k*J*/mole/^{o}K

T = 311.15 ^{o}K

n = number of electrons = 2 for lactate dehydrogenase

F = 96.485 k*J*/mole/*V*

The free cytosolic [NAD^+]/[NADH] calculated from the lactate dehydrogenase reaction:

$$[lactate^-] + [NAD^+] \longrightarrow [pyruvate^-] + [NADH] + [H^+]$$

At pH 7

$$\frac{[\mathrm{Pyr}^-]}{[\mathrm{Lac}^-]} \times \frac{[\mathrm{NADH}]}{[\mathrm{NAD}^+]} = K_{LDH} = 1.11 \times 10^{-4}$$

Rearranged and substituted into equation 1 above

$$\mathrm{E}_{\mathrm{NAD/NADH}} = \mathrm{E}^{\circ}{}_{\mathrm{NAD/NADH}} + \frac{\mathrm{RT}}{\mathrm{nF}} \ln\left(\frac{\mathrm{Pyr}^-}{\mathrm{Lac}^-} \times \frac{1}{\mathrm{K}_{\mathrm{LDH}}}\right)$$

For [pyruvate]/[lactate] = 1:1

$$\mathrm{E}_{\mathrm{NAD/NADH}} = -0.32V + 0.122\mathrm{V} = -0.198\mathrm{V}$$

For [pyruvate]/[lactate] = 1:10

$$\mathrm{E}_{\mathrm{NAD/NADH}} = -0.32V + 0.091\mathrm{V} = -0.229\mathrm{V}$$

The free cytosolic [$NADP^+$]/[NADPH] redox potential calculated from isocitrate dehydrogenase reaction and from the malic enzyme agree well and are the most negative potential in the cell, although with improved metabolite measurements are slightly above the −0.42V estimated in the original Krebs and Veech paper (Krebs, 1969).

The redox potential from isocitrate dehydrogenase reaction:

$$\mathrm{E}_{\mathrm{NADP/NADPH}} = \mathrm{E}^{\mathrm{o}}{}_{\mathrm{NADP/NADPH}} + \frac{\mathrm{RT}}{\mathrm{nF}} \ln\left(\frac{\mathrm{NADP}^+}{\mathrm{NADPH}}\right)$$

$$[\mathrm{Isocitrate}^{-3}] + [\mathrm{NADP}^+] \longrightarrow [\alpha\text{–Ketoglutarate}^{2-}] + [\mathrm{NADPH}] + [\mathrm{CO}_2]$$

$$\frac{[\mathrm{NADP}^+]}{[\mathrm{NADPH}]} = \frac{[\alpha\mathrm{KG}^{2-}] \times [\mathrm{CO}_2]}{[\mathrm{Isocit}^{3-}]} \times \frac{1}{\mathrm{K}_{\mathrm{ICDH}}}$$

$$\mathrm{E}_{\frac{\mathrm{NADP}}{\mathrm{NADPH}}} = \mathrm{E}^{\mathrm{o}}{}_{\frac{\mathrm{NADP}}{\mathrm{NADPH}}} + \frac{\mathrm{RT}}{\mathrm{nF}} \ln\left(\frac{[\alpha\mathrm{KG}^{2-}] \times [\mathrm{CO}_2]}{[\mathrm{Isocit}^{3-}]} \times \frac{1}{\mathrm{K}_{\mathrm{ICDH}}}\right)$$

For [α-Ketoglutarate]:[Isocitrate] = 7:1 (Liver) and [CO_2] = 1.985mM

$$\mathrm{E}_{\frac{\mathrm{NADP}}{\mathrm{NADPH}}} = -0.32V - 0.044\mathrm{V} = -0.364\mathrm{V}$$

The redox potential from from the malic enzyme reaction:

$$\frac{[\mathrm{NADP}^+]}{[\mathrm{NADPH}]} = \frac{[\mathrm{Pyr}^-] \times [\mathrm{CO}_2]}{[\mathrm{Mal}^{2-}]} \times \frac{1}{\mathrm{K}_{\mathrm{MalEnz}}}$$

where [pyruvate]/[malate] = 1:3 in liver

$$\mathrm{E}_{\frac{\mathrm{NADP}}{\mathrm{NADPH}}} = -0.32V - 0.055\mathrm{V} = -0.375\mathrm{V}$$

Because the glutathione couple reacts with the NADP- couple (see Table 27.3), the potential of the NADP- couple determines the redox potential of the glutathione redox couple $[GSH]^2$/[GSSG]) with which it is in near-equilibrium at −0.37V, not the standard potential of −0.32V at pH 7.0. The terminal reduction of the oxygen free radicals involves glutathione, which constitutes the most abundant intracellular antioxidant at 5 mM (Krebs, 1969).

Table 27.3 Enzymatic Systems Which Assume the Redox Potential of the NADP-System

Enzyme	Reaction
Glutathione Reductase EC 1.6.4.2	$NADPH + GSSG + H^+ \rightarrow NADP^+ + 2GSH$
Glutathione Dehydrogenase EC 1.8.5.1	$2GSH + Dehydroascorbate \rightarrow GSSG + Ascorbate$
Glutathione Peroxidase EC 1.11.1.9	$2GSH + H_2O_2 \rightarrow GSSG + H_2O$
Glutathione Transferase EC 2.5.1.8	$HO - Xenobiotic + GSH \rightarrow GS - Xenobiotic + H_2O$
Thioredoxin Reductase EC 1.6.4.5	$NADPH + H^+ + OxidizedThioredoxin \rightarrow NADP^+ + ReducedThioredoxin$

Ascorbate, at 2–3 mM, is the second most abundant reducing agent and antioxidant, and is also the cofactor for a number of metal-dependent oxygenases and dioxygenases, such as collagen prolyl and lysyl hydroxylases (Linster and Van Schaftingen, 2007). Ascorbate, when acting as a reducing agent, loses an electron and a proton to form semidehydroascorbate (SDA), which upon losing another electron forms dehydroascorbate (DHA). Regeneration of ascorbate by glutathione occurs by the reaction: *DHA + 2GSH ↔ ascorbate + GSSG*, which can occur spontaneously (Linster and Van Schaftingen, 2007) but can also be catalyzed by the enzyme glutathione dehydrogenase (EC 1.8.5.1), an enzyme with an activity in rat liver of about 3 µmol/min/g wet weight (Carlberg and Mannervik, 1975). These reactions (Table 27.3) ensure that the redox potential of ascorbic acid and the glutathione couple in vivo assume the redox potential of the cytosolic NADP- couple of −0.37 V and not the standard potential—this is in sharp contrast to ascorbate's standard reduction potential of −0.06 V (Table 27.4) or the standard potential of the glutathione couple at −0.23 V (Clark, 1960).

Table 27.4 Redox Potential of Some Biochemically Important Half-Reactions in the Biochemical Half Reactions, All Reactants Are at 1 M except H^+ Which Is at pH 7.

Half reaction	**Redox Potential of half reactions**
$H^+ + e^- \rightarrow \frac{1}{2} H_2$	-0.41
$\text{Acetyl} - \text{CoA} + 2H^+ + 2e^- \rightarrow \text{Acetaldehyde} + \text{CoA}$	–0.42
$\text{Acetoacetate}^- + 2H^+ 2e^- \rightarrow \beta - \text{hydroxybutyrate}^-$	–0.36
$NAD^+ + 2H^+ + 2e^- \rightarrow NADH + H^+$	–0.32
$NADP^+ + 2H^+ + 2e^- \rightarrow NADPH + H^+$	–0.32
α ketoglutarate^{2-} + $CO_2 + 2H^+ + 2e^- \rightarrow$ isocitrate^{3-}	–0.318
$\text{Pyruvate} + 2H^+ + 2e^- \rightarrow \text{Lactate}$	–0.19
$FAD + 2H^+ + 2e^- \rightarrow FADH_2$	–0.06
$\text{Fumarate} + 2H^+ + 2e^- \rightarrow \text{Succinate}$	+0.031
$\text{Dehydroascorbate} + 2H^+ + 2e^- \rightarrow \text{Acorbate}$	+0.06
$\alpha - \text{ketoglutarate}^{2-} + CO_2 \rightarrow \text{isocitrate}^{3-}$	+0.002
$\text{Ubiquinone} + 2H^+ + 2e^- \rightarrow \text{Dihydroubiquinone}$	+0.10
$\frac{1}{2} O_2 + H_2O + 2e^- \rightarrow H_2O_2$	+0.30
$O_2 + 2H^+ + 2e^- \rightarrow H_2O_2$	+0.605
$Fe^{3+} + e^- \rightarrow Fe^{2+}$	+0.77
$\frac{1}{2} O_2 + H^+ + 2e^- \rightarrow H_2O$	+0.816
$O_{2^-} + 2H^+ \rightarrow H_2O_2$	+0.89

$\bullet OH + e^- \rightarrow OH^-$	+1.89

The semidehydroascorbte (SDA) is also reduced to ascorbate by thioredoxin reductase (EC 1.6.4.5) (Linster and Van Schaftingen, 2007), an NADP-linked enzyme that is the major cellular protein disulfide reductase (Arner and Holmgren, 2000). This enzyme catalyzes the reaction: $NADPH + thioredoxin_{ox} \rightarrow NADP^+ + thioredoxin_{red}$. This enzyme is critical in signaling as part of thiol redox control, and regulates the activity of a number of transcription factors. The potential of the thioredoxin system is likewise set by the potential of the free cytosolic [$NADP^+$]/[NADPH] couple.

Thus, the potential of the ascorbate couple and the glutathione couple are the same as that of the NADP- couple. Likewise, disulfide (SS) groups in protein are reduced to –SH by the thioredoxin system.

The Redox State of Oxygen Free Radicals and Other Relevant Reactants

A list of relevant redox potentials is listed in Table 27.4 below. The values for the redox potentials given are taken from Bergman et al. (2010), Clark (1960), Dawes (1971), and Krebs (1969).

This table shows the oxidizing potential of ROS compounds. However, it should be pointed out that these half reactions do not represent the redox potential inside of cells, which are set by the NAD and NADP couples which carry the dominant metabolic flux during metabolism.

How D-BHB Alters Cellular Redox States

The effects of insulin, glucose, and D-β-hydroxybutyrate (D-βHB) on a perfused rat heart gave insights into the changes in relative concentrations of key metabolites involved in the Krebs cycle and oxidative phosphorylation and the free [$NADP^+$]/[NADPH] ratio. Prior work on the effects of hearts perfused with D-βHB showed that the [isocitrate]/[α-ketoglutarate] (Sato et al., 1995) couple was increased. This change indicated a reduction of the NADP- couple (Kashiwaya et al., 1997). Figure **27.5** shows the increased ratio of [NADPH]/[$NADP^+$] found in the perfused rat heart studies, which supports a highly significant increase in the capacity for cellular ROS/RNS detoxification. (We are intentionally breaking a long-standing rule by putting the reduced form in the numerator to simplify the discussion where an increase in [NADP+]/[NADPH] would otherwise be reported as a decrease in the inverse of the ratio.)

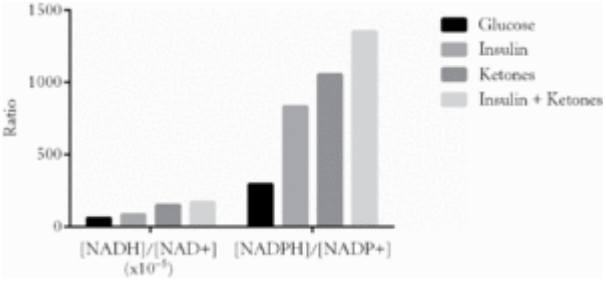

Figure 27.5
Studies of a perfused rat heart demonstrated that the ketone body D-βOHB raised the ratio of [NADPH]/[NADP+]. Modified presentation of data published in Kashiwaya et al. 1997.

Figure **27.6** shows some of the “NADP system” that is relevant to removal of ROS and RNS as well as the link back to D-βHB.

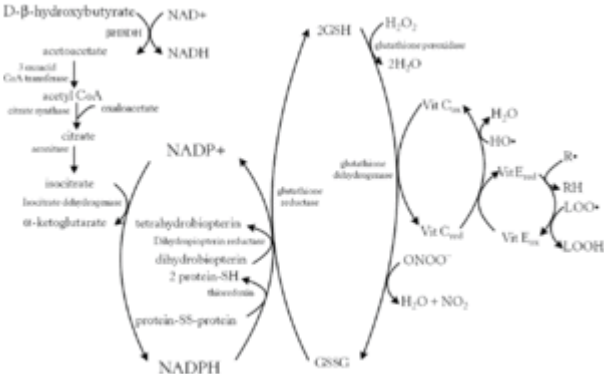

Figure 27.6
The “NADP system” is driven by the [NADP+]/[NADPH] couples redox potential. [NADPH] was elevated relative to [NADP+] in perfused rat heart studies with d-bOHB. To the left of NADPH shown in the diagram is the relevant pathway to reducing NADP+ to NADPH. NADPH also provides the reducing potential to counteract ROS and RNS through antioxidants that must be reduced each time they are oxidized as they quench a ROS or RNS. Abbreviations: NAD—nicotinamide adenine dinucleotide, NADH—reduced NAD+, NADP—nicotinamide adenine dinucleotide phosphate, NADPH—reduced NADP+, GSH—glutathione, GSSG glutathione disulfide, Vit C—vitamin C or ascorbate, Vit E—vitamin E or a tocopherol, R•—free radical on a carbon atom, RH—an organic molecule with C-H bond, LOO•—lipid peroxyl radical, LOOH—lipid peroxide.

Ketosis as a Means of Protection against Ionizing Radiation

At present there are very few approved treatments for exposure to nuclear accidents or rogue nuclear bombs (Buddemeier, 2011). Experiments have been conducted at the Armed Forces Radiobiology Research Institute (AFRRI). The study investigating D-βHB protection against acute ROS injury utilized in vitro radiation lethality on HOS (human osteoblast) cells exposed to several doses and types of radiation. For the studies described below, a novel ester of D-β-hydroxybutyrate and R-1,3-butanediol referred to as ketone ester (KE), was used. This compound has been shown to safely increase levels of blood D-βHB to 5–7 mM (Clarke et al., 2012a; Clarke et al., 2012b). The ester is hydrolyzed in the gut and blood by esterases, and the resulting *R*-1,3 butane diol is converted to D-βHB in the liver (Figure **27.7**).

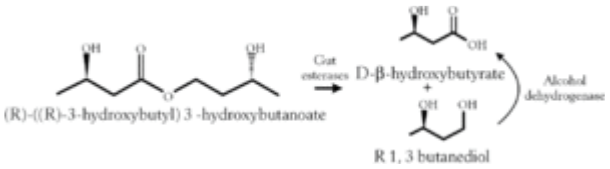

Figure 27.7
The monoester of D-βOHB and R-1,3 butanediol is (R)-((R)3-hydroxybutyl) 3- hydroxybutyrate is converted to two molecules of D-βOHB and provides an alternative fuel to produce ATP.

The Removal of Free Radicals in Vivo

Clinical trials of administration of antioxidants have often been disappointing (Winterbourn, 2008). Most placebo trials of antioxidants have failed (Steinhubl, 2008), most notably in the long-advocated use of high-dose ascorbic acid. The use of vitamin antioxidants has not objectively been proven helpful in the absence of vitamin deficiency and may even be harmful (Howes, 2011). More recently, high doses of Vitamin E are reported to increase melanoma metastases in mice (LeGal, 2015).

While it is true that, quantitatively, glutathione at about 5 mM and ascorbic acid at about 2–3 mM in most cells are the predominant intracellular antioxidants, one cannot change the redox potential of an antioxidant in vivo by simply adding more of the reduced form of the couple.

Removal of Reactive Oxygen Species by Generation of NADPH

We have discussed earlier the failure to remove ROS by addition of antioxidants such as ascorbic acid (Steinhubl, 2008). It is likewise not possible to add the reduced component of most NADPH producing metabolite couples (see Table 27.2 above), since these multiply-charged compounds do not readily enter the interior of cells. It is, however, possible to introduce the reduced ketone body, D-βHB, which readily enters cells on the monocarboxylate transporter, MCT. While not an NADP- coupled metabolite, D-βHB produces acetyl CoA and, via the Krebs cycle, increased concentrations of citrate and isocitrate, but causes little change in α-ketoglutarate (Sato et al., 1995). This increase in the [isocitrate]/[α-ketoglutarate] ratio causes a reduction of the NADP- system (Kashiwaya et al., 1997) generated by the metabolism involving the most active NADP linked dehydrogenase, isocitrate dehydrogenase. The cellular metabolic processes thus produce an increased reducing power of the NADP system, which is regenerated by the cellular metabolism.

The Enzymes Destroying Reactive Oxygen Species

Superoxide dismutase also can combine two superoxide radicals, along with two protons to form the less toxic hydrogen peroxide.

$$O_{2^-} + O_{2^-} + 2H^+ \rightarrow H_2O_2 + O_2$$

Hydrogen peroxide can react with catalase (EC 1.11.1.6) in cytoplasm, but not mitochondria, to form water and O_2.

$$2H_2O_2 \rightarrow O_2 + 2H_2O$$

Alternatively, H_2O_2 can react with glutathione in a reaction catalyzed by glutathione peroxidase (EC 1.11. 1.9) to form oxidized glutathione and water.

$$2GSH + H_2O_2 \rightarrow GSSG + 2H_2O$$

The Effects of D-BHB on Transcription

In addition to the ability of D-βHB metabolism to generate NADPH, the metabolite D-βHB is the natural inhibitor of class I and II histone deacetylases (Shimazu et al., 2013; Veech, 2014) that were formerly identified by their ability to bind nicotinic acid (Offermanns, 2006; Tunaru et al., 2003). The inhibition of histone deacetylase increases transcription of the enzymes of the antioxidant pathway controlled by the

FOXO3A and Mt1 transcription factors, thus increasing the activity of Mn superoxide dismutase and catalase (see Table 27.3). D-βHB thus increases the reductive capacity of the pathways used to destroy free radicals by increasing the enzymes in the pathway used for free radical destruction. Recent studies have shown that HDAC inhibitors may have a significant benefit in radiation protections (Brown et al., 2008; Miller et al., 2011). Therefore, in vitro studies were initiated to test whether KE could improve radiation survival and decrease radiation-induced damage.

In Vitro Studies

Human osteoblast cells (HOS) were chosen as the model system to study KE's potential as a radiation countermeasure. The HOS cells have been previously used to evaluate potential radiation countermeasures (Miller et al., 1998; Miller et al., 2011). The HOS cells were incubated with KE (50 μM, 15 min to 1 h) either before (Figure **27.8A**) or immediately after (Figure **27.8B**) exposure to gamma radiation (^{60}Co, 0.66 cGy/min). Following radiation, HOS cells were plated in 100-mm petri dishes to assess survival of colony-forming cells; at 10 days post radiation, colonies were fixed, stained, and counted to determine the survival fraction. The survival curves show that KE increased survival when delivered either immediately before or immediately after radiation. These data strongly suggest that KE would have benefit to human health both as a protectant delivered to populations at risk of exposure or as a mitigant after radiation. The ability of KE to improve survival even when given 24 hours after radiation is compatible with the persistent production of superoxide from NADPH oxidase s, DUOX 1 and 2, for several days after radiation exposure (Ameziane-El-Hassani et al., 2015).

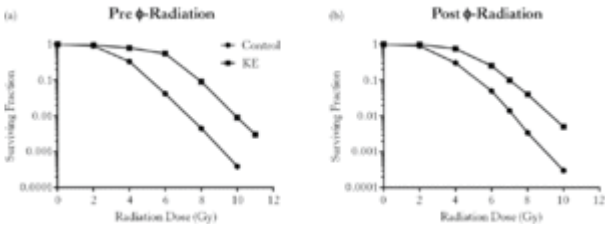

Figure 27.8
Survival curves for human osteoblasts (HOS) in culture exposed to either gamma (60Co, 66 gCy/min) or proton radiation (4MeV). KE-treated cell cultures received 50 μM of ketone ester (KE) in the cell media 30 minutes prior to or for 30 minutes after radiation exposure.

Proton radiation was used to determine the ability of the KE to protect against particle radiation, which produces less oxidative damage than

gamma radiation but is more likely to induce double-stranded DNA breaks (Lomax et al., 2013). Cells were exposed to KE before proton radiation exposure, similar to that performed above in Figure **27.8A** with gamma radiation. The KE was able to confer significant protection against proton radiation in this model (Figure **27.8C**). Overall cell death was higher for this type of radiation, which is to be expected, based on previous studies. Protection against proton radiation is of particular interest to NASA, as astronauts have a substantially greater likelihood of exposure to proton radiation than other populations.

Genomic effects of ROS begin as discrete events such as a break in the phosphate backbone in DNA, nitrogenous base oxidation, or dimerization. Breaks in the phosphate bonds occur as either single, clustered, or double-stranded breaks, depending on the level of the ROS or radiation dose and type. As the frequency of breaks increases, macro effects such as abnormal chromosomes, mutagenesis, and inhibited cell division become more frequent (Lomax et al., 2013). In general, single-stranded breaks are quickly repaired, have low cytotoxicity and occur at high levels even without exogenous ROS or radiation (Cadet et al., 2008). Single-stranded breaks are induced at levels four- to eightfold more than double-stranded breaks with exposure to electromagnetic radiation such as gamma or x-rays (Lomax et al., 2013). Double-stranded or clustered single-stranded breaks occur with particle radiation, especially α and proton, or when ROS is focused in a confined area (Lomax et al., 2013). A double-stranded break is defined as two breaks within 10 bases (Lomax et al., 2013). These breaks are much more difficult to repair and can persist for more than 24 hours when large numbers are generated (Schmid et al., 2010). These breaks are repaired by either homologous recombination or by nonhomologous end joining (Lomax et al., 2013), with the latter being the predominant mechanism in most phases of the cell cycle. It is possible to observe these breaks by examining some of the hallmarks of their repair, by observing different types of aberrant chromosomes, or by observing cell cycle arrest. Indeed, when cultured cells were treated with D-βHB before an exposure to γ radiation, production of chromosomal aberrations and cell cycle arrest were both significantly suppressed (Figure **27.9**).

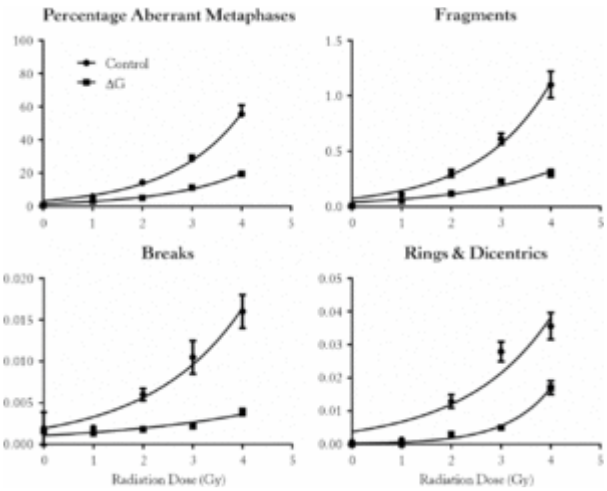

Figure 27.9
The percentage of chromosomal anomalies (aberrant metaphases, fragments, breaks, and rings and dicentrics) occurring from γ-radiation-exposed human osteoblast cells (HOS) with or without KE. The 50-μM KE was added to the cell culture media 30 minutes prior to radiation exposure and removed immediately prior to radiation exposure. Cells were scored using a light microscope.

A novel approach for stimulating repair of radiation or ROS-induced DNA damage utilizes HDAC inhibitors. Inhibitors of HDAC activate important DNA repair pathways such as the Nrf2 and Rad51 and decrease markers of damage, even if the inhibitor is given after radiation exposure (Brown et al., 2008; Miller et al., 2011). Histone deacetylase (HDAC) inhibitors have broad activity, their primary function is to increase the acetylation of histones by preventing their deacetylation, in turn making the genome less tightly packed and more transcriptionally active (Verdin and Ott, 2015). The deacetylating activity of HDACs can also extend to various other cellular proteins, modulating activity of enzymes and protein-protein binding (Verdin and Ott, 2015). With huge numbers of potential effects resulting from inhibiting HDACs, it is difficult to determine what the final effectors of the protection are, but studies have demonstrated that a series of chemically unrelated compounds that all target HDACs seem to confer similar protection and enhanced repair after exposure (Brown et al., 2008; Miller et al., 2011; Shimazu et al., 2013).

The effects of persistent DNA damage are most quickly seen in tissues with high cell turnover that rely on actively dividing stem cells such as skin, the gastrointestinal system, and blood. Damage in these systems produces some of the rapid and most visible radiation effects, such as

hair loss, nausea/vomiting, bone marrow suppression, and skin lesions. Damage to DNA is also responsible for much of the increased risk of cancer that results from radiation exposure.

Effects of Ketone Esters after Exposure to Radiation in Vivo

A project is underway to evaluate the ability of KE to increase murine survival after gamma radiation exposure. Previous studies have shown that exposure of the DBA2 inbred mouse strain to 6 Gy of γ-radiation results in reproducible bone marrow chromosomal damage in 85-day-old mice (Grahn, 1958). In our study we have tested a single KE administration of 750 mg/kg by gavage 24 hours after radiation exposure. This postradiation treatment led to a consistent 50% decrease in numerous types of radiation-induced chromosomal malformations and abnormal cell divisions as observed by microscopy 24 hours after KE administration (Figure **27.10**). The importance of decreasing these indicators of DNA damage and genomic instability is underscored by the cytotoxicity of this type of damage and the potential for neoplastic transformation, ultimately resulting in cancer. This dose of KE also blunted the radiation-induced increase in incidence of micronuclei, which arise from improper chromatid separation during anaphase, in both reticulocytes and erythrocytes, which were counted using the methods of Schmid (1975).

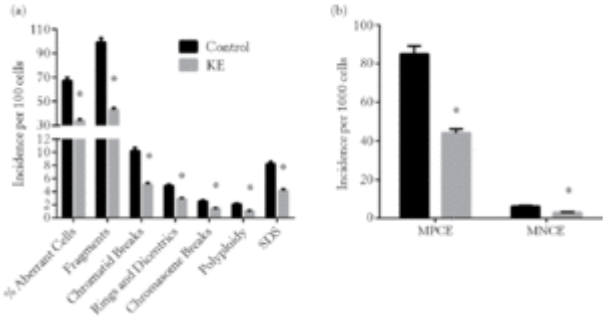

Figure 27.10
The effect of KE on the incidence rate of chromosome anomalies and micronuclei in mouse bone marrow 48 h after 6 Gy γ-radiation. KE (750 mg/kg) or saline were delivered by gavage 24 hours after radiation exposure. (A) Chromosomal malformation incidence per 100 cells, all cells in bone marrow were examined and malformations were scored using a light microscope. For metaphases approximately 1,000 total were counted, 200/animal. (B) Micronuclei were counted only in reticulocytes and erythrocytes, 10,000 total were counted per animal.

Data presented as average ± SEM, $N = 5$ animals, *, $p < .01$ by t-test with a Sidack-Bonferonni multiple comparison correction.

In order to explore KE effects on radiation bone marrow suppression and impact on hematopoiesis, an important mechanism for radiation-induced mortality at the 6 Gy level, the ratio between total reticulocytes and erythrocytes in bone marrow was determined. Bone marrow was extracted as before, 24 hours after KE or saline gavage, a total of 48 hours after either 0.5 or 6 Gy γ-radiation. This ratio, which is approximately 1 in bone marrow under normal circumstances, was significantly decreased by both 0.5 and 6 Gy doses of γ-radiation (Figure **27.11**) in control animals. This decrease was significantly attenuated by 750mg/kg KE 24 hours after radiation. Further experiments to determine KE effects on radiation lethality are ongoing.

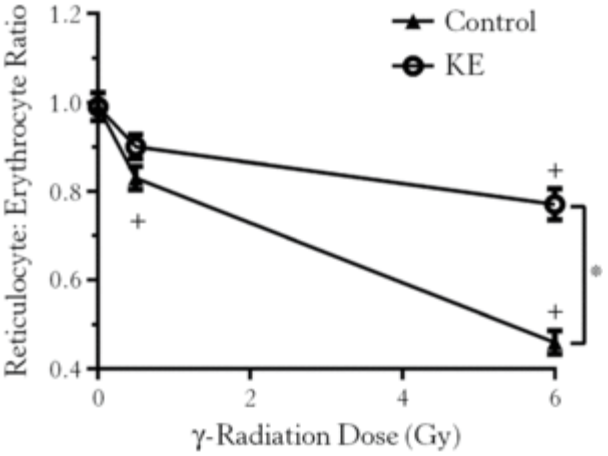

Figure 27.11
The effect of KE on the relative abundance of polychromatic and normochromatic erythrocytes in mouse bone marrow 48 h after 0, 0.5, or 6 Gy γ-radiation. KE (750 mg/kg) or saline were delivered by gavage 24 hours after radiation exposure. 10,000 erythrocytes were counted per animal.

Data presented as average ± SEM, $N = 5$ animals. *, $p < .01$ significant difference between KE and control, +, $p < 0.05$ significant difference versus no radiation, by t-test with a Sidack-Bonferonni multiple comparison correction.

Conclusion

Reactive oxygen species play a central role in both radiation damage and aging. It is proposed that both processes can be ameliorated by the administration of KE to increase the amount of antioxidant, enzymes, and the reducing power of the NADP- system.

References

Acquier, A.B., Mori Sequeiros Garcia, M., Gorostizaga, A.B., Paz, C., and Mendez, C.F. (2013). Reactive oxygen species mediate dopamine-induced signaling in renal proximal tubule cells. FEBS Lett 587, 3254–3260.

Ameziane-El-Hassani, R., Talbot, M., de Souza Dos Santos, M.C., Al Ghuzlan, A., Hartl, D., Bidart, J.M., De Deken, X., Miot, F., Diallo, I., de Vathaire, F., et al. (2015). NADPH oxidase DUOX1 promotes long-term

persistence of oxidative stress after an exposure to irradiation. Proc Natl Acad Sci U S A 112, 5051–5056.

Arner, E.S., and Holmgren, A. (2000). Physiological functions of thioredoxin and thioredoxin reductase. Eur J Biochem 267, 6102–6109.

Bedard, K., and Krause, K.H. (2007). The NOX family of ROS-generating NADPH oxidases: physiology and pathophysiology. Physiol Rev 87, 245–313.

Ben-Porath, I., and Weinberg, R.A. (2005). The signals and pathways activating cellular senescence. Int J Biochem Cell Biol 37, 961–976.

Bergman, C., Kashiwaya, Y., and Veech, R.L. (2010). The effect of pH and free Mg^{2+} on ATP linked enzymes and the calculation of Gibbs free energy of ATP hydrolysis. J Phys Chem B 114, 16137–16146.

Blackburn, E.H., and Gall, J.G. (1978). A tandemly repeated sequence at the termini of the extrachromosomal ribosomal RNA genes in Tetrahymena. J Mol Biol 120, 33–53.

Brown, S.L., Kolozsvary, A., Liu, J., Ryu, S., and Kim, J.H. (2008). Histone deacetylase inhibitors protect against and mitigate the lethality of total-body irradiation in mice. Radiat Res 169, 474–478.

Bucher, T., and Klingenberg, M. (1958). Wege des Wasserstoffs in der lebendigen Organisation. Angewandte Chemie 70, 552–570.

Buddemeier, B.R. (2011). Key Response Planning Factors for the Aftermath of Nuclear Terrorism (FEMA, Homeland Security, Sandia National Laboratory, Lawrence Livermore National Laboratory).

Burton, K. (1974). The enthalpy change for the reduction of nicotinamide-adenine dinucleotide. Biochem J 143, 365–368.

Cadet, J., Douki, T., and Ravanat, J.L. (2008). Oxidatively generated damage to the guanine moiety of DNA: mechanistic aspects and formation in cells. Acc Chem Res 41, 1075–1083.

Carlberg, I., and Mannervik, B. (1975). Purification and characterization of the flavoenzyme glutathione reductase from rat liver. J Biol Chem 250, 5475–5480.

Chance, B., Sies, H., and Boveris, A. (1979). Hydroperoxide metabolism in mammalian organs. Physiol Rev 59, 527–605.

Clark, W.M. (1960). Oxidation Reduction Potentials of Organic Systems (Baltimore: Williams and Wilkins).

Clarke, K., Tchabanenko, K., Pawlosky, R., Carter, E., Knight, N.S., Murray, A.J., Cochlin, L.E., King, M.T., Wong, A.W., Roberts, A., et al. (2012a). Oral 28-day and developmental toxicity studies of (R)-3-hydroxybutyl (R)-3-hydroxybutyrate. Regul Toxicol Pharmacol 63, 196–208.

Clarke, K., Tchabanenko, K., Pawlosky, R., Carter, E., Todd King, M., Musa-Veloso, K., Ho, M., Roberts, A., Robertson, J., Vanitallie, T.B., et al. (2012b). Kinetics, safety and tolerability of (R)-3-hydroxybutyl (R)-3-hydroxybutyrate in healthy adult subjects. Regul Toxicol Pharmacol 63, 401–408.

Correia-Melo, C., Hewitt, G., and Passos, J.F. (2014). Telomeres, oxidative stress and inflammatory factors: partners in cellular senescence? Longev Healthspan 3, 1.

Dawes, E.A. (1971). Quantitative problems in biochemistry, Vol. 3, 5th edition (Edinburgh & London: E. & S. Livingstone).

Grahn, D. (1958). Acute radiation response of mice from a cross between radiosensitive and radioresistant strains. Radiat Res 4, 189–198.

Harley, C.B., Futcher, A.B., and Greider, C.W. (1990). Telomeres shorten during ageing of human fibroblasts. Nature 345, 458–460.

Harman, D. (1956). Aging: a theory based on free radical and radiation chemistry. J Gerontol 11, 298–300.

Harman, D. (1981). The aging process. Proc Natl Acad Sci USA 78, 7124–7128.

Holzer, H., Schultz, G., and Lynen, F. (1956). Bestimmung des quotienten DPNH/DPN in lebenden hefezellen durch analyse stationarer alkohol und acetaldehyde konzentrationen. Biochem Z 332, 252–263.

Howes, R. (2011). Mythology of antioxidant enzymes. J Evidence Based Compl Altern Med 16, 149–159.

Kashiwaya, Y., King, M.T., and Veech, R.L. (1997). Substrate signaling by insulin: a ketone bodies ratio mimics insulin action in heart. Am J Cardiol 80, 50A–64A.

Kashiwaya, Y., Takeshima, T., Mori, N., Nakashima, K., Clarke, K., and Veech, R.L. (2000). D-beta-Hydroxybutyrate protects neurons in models of Alzheimer’s and Parkinson’s disease. Proc Natl Acad Sci USA 97, 5440–5444.

Krebs, H.A., and Veech, R.L. (1969). Pyridine nucleotide interrelations. In The Energy Level and Metabolic Control in Mitochondria, S. Papa, Tager, J.M., Quagliariello, E., & Slater, E.C., eds. (Bari, Italy: Adriatica Editrice), pp. 329–384.

LeGal, K. (2015). Antioxidants can increase melanoma metastasis in mice. Sci Transl Med 7, 1–7.

Linster, C.L., and Van Schaftingen, E. (2007). Vitamin C: biosynthesis, recycling and degradation in mammals. FEBS J 274, 1–22.

Lomax, M.E., Folkes, L.K., and O'Neill, P. (2013). Biological consequences of radiation-induced DNA damage: relevance to radiotherapy. Clin. Oncol. 25, 578–585.

Miller, A.C., Blakely, W.F., Livengood, D., Whittaker, T., Xu, J., Ejnik, J.W., Hamilton, M.M., Parlette, E., John, T.S., Gerstenberg, H.M., et al. (1998). Transformation of human osteoblast cells to the tumorigenic phenotype by depleted uranium-uranyl chloride. Environ Health Perspect 106, 465–471.

Miller, A.C., Cohen, S., Stewart, M., Rivas, R., and Lison, P. (2011). Radioprotection by the histone deacetylase inhibitor phenylbutyrate. Radiat Environ Biophys 50, 585–596.

Mourkioti, F., Kustan, J., Kraft, P., Day, J.W., Zhao, M.M., Kost-Alimova, M., Protopopov, A., DePinho, R.A., Bernstein, D., Meeker, A.K., et al. (2013). Role of telomere dysfunction in cardiac failure in Duchenne muscular dystrophy. Nat. Cell Bio 15, 895–904.

Offermanns, S. (2006). The nicotinic acid receptor GPR109A (HM74A or PUMA-G) as a new therapeutic target. Trends Pharmacol Sci 27, 384–390.

Olovnikov, A.M. (1973). A theory of marginotomy. The incomplete copying of template margin in enzymic synthesis of polynucleotides and biological significance of the phenomenon. J Theor Biol 41, 181–190.

Opresko, P.L., Fan, J., Danzy, S., Wilson, D.M., 3rd, and Bohr, V.A. (2005). Oxidative damage in telomeric DNA disrupts recognition by TRF1 and TRF2. Nucleic Acids Res 33, 1230–1239.

Orr, W.C., Radyuk, S.N., and Sohal, R.S. (2013). Involvement of redox state in the aging of Drosophila melanogaster. Antioxid Redox Signal 19, 788–803.

Pacher, P., Beckman, J.S., and Liaudet, L. (2007). Nitric oxide and peroxynitrite in health and disease. Physiol Rev 87, 315–424.

Pham-Huy, L.A., He, H., and Pham-Huy, C. (2008). Free radicals, antioxidants in disease and health. Int J Biomed Sci 4, 89–96.

Sato, K., Kashiwaya, Y., Keon, C.A., Tsuchiya, N., King, M.T., Radda, G.K., Chance, B., Clarke, K., and Veech, R.L. (1995). Insulin, ketone bodies, and mitochondrial energy transduction. FASEB J 9, 651–658.

Schmid, T.E., Dollinger, G., Beisker, W., Hable, V., Greubel, C., Auer, S., Mittag, A., Tarnok, A., Friedl, A.A., Molls, M., et al. (2010). Differences in the kinetics of gamma-H2AX fluorescence decay after exposure to low and high LET radiation. Int J Radiat Biol 86, 682–691.

Schmid, W. (1975). The micronucleus test. Mutation Research 31, 9–15.

Schriner, S.E., Linford, N.J., Martin, G.M., Treuting, P., Ogburn, C.E., Emond, M., Coskun, P.E., Ladiges, W., Wolf, N., Van Remmen, H., et al. (2005). Extension of murine life span by overexpression of catalase targeted to mitochondria. Science 308, 1909–1911.

Schrodinger, E. (1944). What Is Life Mind and Matter (Cambridge, UK: Cambridge University Press).

Scott, E.M., Duncan, I.W., and Ekstrand, V. (1963). Purification and properties of glutathione reductase of human erythrocytes. J Biol Chem 238, 3928–3933.

Sfeir, A. (2012). Telomeres at a glance. J Cell Sci 125, 4173–4178.

Shimazu, T., Hirschey, M.D., Newman, J., He, W., Shirakawa, K., Le Moan, N., Grueter, C.A., Lim, H., Saunders, L.R., Stevens, R.D., et al. (2013). Suppression of oxidative stress by beta-hydroxybutyrate, an endogenous histone deacetylase inhibitor. Science 339, 211–214.

Sohal, R.S., and Weindruch, R. (1996). Oxidative stress, caloric restriction, and aging. Science 273, 59–63.

Speakman, J.R. (2005). Body size, energy metabolism and lifespan. J Exp Biol 208, 1717–1730.

Steinhubl, S.R. (2008). Why have antioxidants failed in clinical trials? Am J Cardiol 101, 14D-19D.

Szilard, L. (1959). On the nature of the aging process. Proc Natl Acad Sci USA 45, 30–45.

Tunaru, S., Kero, J., Schaub, A., Wufka, C., Blaukat, A., Pfeffer, K., and Offermanns, S. (2003). PUMA-G and HM74 are receptors for nicotinic acid and mediate its anti-lipolytic effect. Nat Med 9, 352–355.

Veech, R.L. (2005). Mitochondrial bioenergetics in intact tissues. In Mitochondria in Health and Disease, C.D. Berdanier, ed. (New York: CRC Press, Taylor & Francis), pp. 65–94.

Veech, R.L. (2006). The determination of the redox states and phosphorylation potential in living tissues and their relationship to metabolic control of disease phenotypes. Biochem Mol Biol Edu 34, 168–179.

Veech, R.L. (2014). Ketone ester effects on metabolism and transcription. J Lipid Res 55, 2004–2008.

Veech, R.L., Eggleston, L.V., and Krebs, H.A. (1969). The redox state of free nicotinamide-adenine dinucleotide phosphate in the cytoplasm of rat liver. Biochem J 115, 609–619.

Veech, R.L., Lawson, J.W.R., Cornell, N.W., and Krebs, H.A. (1979). Cytosolic phosphorylation potential. Journal of Biological Chemistry 254, 6538–6547.

Verdin, E., and Ott, M. (2015). 50 years of protein acetylation: from gene regulation to epigenetics, metabolism and beyond. Nat Rev Mol Cell Biol 16, 258–264.

Villet, R.H., and Dalziel, K. (1969). The nature of the carbon dioxide substrate and equilibrium constant of the 6-phosphogluconate dehydrogenase reaction. Biochem J 115, 633–638.

von Zglinicki, T. (2002). Oxidative stress shortens telomeres. Trends in Biochemical Sciences 27, 339–344.

Williamson, D. H., Lund, P., & Krebs, H. A. (1967). The redox state of free nicotinamide-adenine dinucleotide in the cytoplasm and mitochondria of rat liver. Biochem J, 103(2), 514–527.

Winterbourn, C.C. (2008). Reconciling the chemistry and biology of reactive oxygen species. Nat Chem Biol 4, 278–286.

Wollenberger, A., Ristau, O., and Schoffa, G. (1960). Eine einfache Technik der extrem schnellen Abkuhlung grssáerer Gewebestacke. Pflugers Archiv 270, 399–412.

Yamato, M., Kudo, W., Shiba, T., Yamada, K.I., Watanabe, T., and Utsumi, H. (2010). Determination of reactive oxygen species associated with the degeneration of dopaminergic neurons during dopamine metabolism. Free Radic Res 44, 249–257.

Notes:

* Authors contributed equally.